INSTITUTE FOR FUSION STUDIES

DOE/ET-53088-532 IFSR #532

Comparisons of Theoretically Predicted Transport from Ion Temperature Gradient Instabilities to *L*-Mode Tokamak Experiments

M. KOTSCHENREUTHER, H.V. WONG, P.L. LYSTER,
H.L. BERK, R. DENTON, W.H. MINER, and P. VALANJU
Institute for Fusion Studies
The University of Texas at Austin
Austin, Texas 78712

December 1991

THE UNIVERSITY OF TEXAS

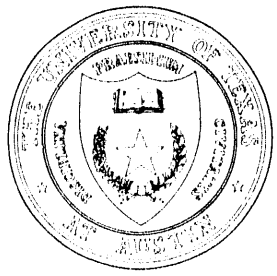

AUSTIN

DISCLAIMER

Comparisons of Theoretically Predicted Transport from Ion Temperature Gradient Instabilities to L-Mode Tokamak Experiments

DOE/ET/53088--532

DE92 006881

M. Kotschenreuther, H.V. Wong, P.L. Lyster,
H.L. Berk, R. Denton, W.H. Miner,
and P. Valanju
Institute for Fusion Studies
The University of Texas at Austin
Austin, Texas 78712

Abstract

The theoretical transport from kinetic micro-instabilities driven by ion temperature gradients in a sheared slab is compared to experimentally inferred transport in L-mode tokamaks. Low noise gyrokinetic simulation techniques are used to obtain the ion thermal transport coefficient χ. This χ is much smaller than in experiments, and so cannot explain L-mode confinement. Previous predictions based on fluid models gave much greater χ than experiments. Linear and nonlinear comparisons with the fluid model show that it greatly overestimates transport for experimental parameters. In addition, disagreements among previous analytic and simulation calculations of χ in the fluid model are reconciled.

Ion temperature gradient driven (ITGD) instabilities are often considered as a possible explanation for anomalous transport in strongly heated tokamak plasma confinement devices, since several qualitative features of the data are roughly consistent with the theoretical properties of ion temperature gradient driven instabilities.[1,2,3] Low noise, nonlinear gyro-kinetic simulation techniques have been developed[4,5,6,7] to examine ITGD turbulence

in sheared magnetic fields in a slab geometry. Predictions for χ from these codes are presented here. The simulation results roughly agree with gyrokinetic mixing length estimates for diffusion D_M, with $\chi \sim 2.5 D_M$. These χ are much too small to explain experimental χ values; we conclude that the slab branch of ITGD instabilities are not responsible for L-mode transport.

Previously, ITGD transport in slab geometry has been considered extensively using fluid models without kinetic effects. Analytic nonlinear theories[8,9,10,11] and numerical simulations[12,13] of (ITGD) transport have been pursued. Unlike the gyro-kinetic results here, the fluid predictions for χ are much larger than experimental χ in the center of the discharge.[3,14,15] The large magnitude of χ from these fluid models has lead to widespread speculation that experiments must be hovering close to marginal stability for these modes.[9,10,14,15,16,17] Experiments to test the marginal stability hypothesis[14] give negative results. In view of these qualitative discrepencies, we will compare the fluid and kinetic models in detail.

Figure 1 shows the theoretical predictions and experimental results from Ref. 3 for the thermal transport coeficient χ in a typical L-mode TFTR discharge (#41309). Note that this discharge is significantly above threshold, $\eta/\eta_c \approx 2 - 4$. The gyrokinetic χ is much smaller than experiment, both for simulation results and linear kinetic mixing length estimates. To obtain the mixing length estimate, linear eigenfunctions were obtained from an integral eigenvalue code with full gyroradius effects. This was cross checked with results in the literature,[18,19] and with simulation results in the linear growth phase from the two independent fully gyrokinetic initial value codes.[4,5,6,7] The frequency and growth rates in all cases agreed to within 5-10%, thereby establishing the accuracy of all the codes. (Further details are given below.)

Fully nonlinear, kinetic 3-d simulations for realistic parameers have also been performed for the slab gyrokinetic equation (accurate to lowest order in the gyrokinetic expansion

parameter)

$$\frac{\partial}{\partial t}\delta f(\mathbf{x}, v_\perp, v_\parallel) + \hat{z} \times \nabla \langle \phi \rangle \cdot \nabla \delta f + v_\parallel \nabla_\parallel \delta f$$

$$v_\parallel \nabla_\parallel \langle \phi \rangle f_M + \left[1 + \eta(v^2 - 3/2)\right] \hat{z} \cdot \nabla \langle \phi \rangle \cdot \hat{x} f_M \qquad (1)$$

where $\delta f = h + q \langle \phi \rangle f_M / T_i$, h is the usual nonadiabatic distribution, time is normalized by ω_{*i}^{-1}, x and y by ρ_i, and $\langle \quad \rangle$ is the gyroaverage.

Two completely different algorithms were used; 1) a δf particle algorithm with greatly reduced noise,[4,5,6] and an implicit spectral algorithm[4,7]

1) Previous particle algorithms have statistical fluctuations in the number of particles per cell, which leads to noise in φ. This can swamp the φ from saturated micro-instabilities.

In the δf particle algorithm,[4,5,7] the nonlinear equation Eq. (1) is solved for δf by integrating the right side along the nonlinear particle orbits (i.e., the method of characteristics). The particle positions are evolved and act as markers for the value of δf. Note that f is related to the full distribution function f and the background f_M by $\delta f = \langle f \rangle - f_M + (\langle \varphi \rangle - \varphi) q f_M / T_i$; thus δf is proportional to the fluctuating amplitude, not the background f_M. The perturbed charge density is computed by accumulating δf on the markers to a grid. Statistical fluctuations in φ are smaller than previous codes by roughly the factor $\delta f / f$; thus the δf algorithm requires orders of magnitude fewer particles to simulate microinstabilities. Since the nonlinear orbit equations preserve phase space volume, no net marker bunching errors arise. For 3-d runs, δf was damped to zero near the boundary to prevent quasilinear flattening.

2) A spectral algorithm which expands the distribution function in basis functions[4,6]: Fourier modes in the x direction, Hermite funtions in x, and a grid in v. Large time steps are possible since the linear terms in the equation are solved implicitly, using analytically derived linear orbit integrals over S for given φ. Also, Hermite functions are close to the linear eigenfunctions, so few are needed. The heat flux out one side in x was reintroduced through the other side, preventing quasilinear flattening.

The simulations had good energy conservation. Also, the saturated fluctuations had correlation widths less than the simulation box size, so that edge effects should not dominate. For the particle algorithm, the box size (for $\eta = 4$) was $x = 21\rho_i$, $y = 25\rho_i$. The wavevector $k_y\,\rho_i = 0.18N$, for $N = 1 - 5$, and there were $5N$ rational surfaces in the simulation volume for each N. The linear modes strongly overlapped for $N > 2$, and significant overlapped for $N = 1$; there was significant nonlinear radial broadening, so that all N strongly overlapped at saturation. Several runs were repeated with $k_y\,\rho_i = 0.1N$, $N = 1 - 5$; relatively little transport was caused by the low k_y modes, and the spectrum rapidly decayed as k_y decreased.

The radial heat flux for Eq. (1) is $\Gamma = \int dv\,\delta f \left(\frac{1}{2}v^2 - 3/2\right)\frac{\partial\langle\phi\rangle}{dy}$. To identify the modes most responsible for transport on average, we note that $\int dxdydz\,\Gamma = \sum_k ik_y\,\langle\phi\rangle_k \int dv\,\delta f_{-k}\cdot\left(\frac{1}{2}v^2 - 3/2\right) \equiv \sum_k Q_k$. The code result for Q_k is shown in Fig. 2 for a time value well after saturation; heat flux is dominated by modes with $k_y\rho \sim 0.4$, slightly less than the most linearly unstable mode. Note that the heat flux rapidly decays away from this peak value.

The spectral code used similar parameters, but only 3 or 4 k_y values could be used due to expense. Though the $|\varphi|^2$ spectrum for the spectral code had decayed less at the cutoff, it still gave results for χ within 40-60% of the δf particle code.

Despite the large difference in the two algorithms, they give transport values roughly close to each other, and roughly consistent with the gyrokinetic D_M. We conclude that the transport in the gyrokinetic model is much less than in experiments.

In Refs. 3,14,15, analytic predictions of the fluid model χ are much larger than experimental χ. Thus, we now compare the fluid and gyro-kinetic model in more detail.

We begin by comparing the linear predictions. Fully gyrokinetic calculations of sheared slab ITGD modes have been performed before,[13,14] but detailed comparisons with fluid models and experiments have not. Multiple independent shooting codes were cross checked for the fluid case. The MFE profile data base was used to obtain profile parameters for many

beam heated L-mode shots. We find that $\eta_i = 4$ and $L_n/L_s = 0.25$ are typical. For the shot shown in Fig. 1, $2.5 < \eta_i < 5.2$ and $0.21 < L_n/L_s < 0.36$ for $0.1 < r/a < 0.6$.

Comparisons of the fluid and kinetic cases are shown in Fig. 3 for the growth rate γ and linear mixing length estimate of the diffusion coeficient $D_M = \gamma \Delta x^2$ (where $\Delta x \equiv \int |\varphi| dx / \int |\partial \varphi / \partial x| dx$ for both cases). We use $k_y \rho_i = 0.4$, which is near the peak of the growth rate and of the saturated spectrum found in Ref. 8 and in fluid simulations.[12,13]

The fluid model overestimates D_M by more than an order of magnitude for typical experimental parameters. Kinetic ion Landau damping is important over the bulk of the eigenfunction. Figure 3 also shows the ratio $R = \omega / v_{\rm th} \left\langle k_{||} \right\rangle$ (where $\left\langle k_{||} \right\rangle = \int |\varphi k_{||}| dx / \int |\varphi| dx$). For fluid theories to be valid, $R \gg 1$ must hold; however $R \tilde{<} 1$ for experimental parameters, and $R \lesssim 2$ even for $\eta_i = 14$.

For the parameters of Fig. 3, higher radial mode numbers $\ell > 0$ have D_M equal or greater than the $\ell = 0$ mode in the fluid case, and cause even greater transport;[9] however, for $\eta_i \sim 4$ and $L_n/L_s \sim 0.25$ the kinetic eigenfunctions for $\ell > 0$ have lower γ and D_M than the $\ell = 0$ mode, due to strong Landau damping.

In Ref. 17, a kinetic calculation was given of χ near marginal stability, and χ was found to be much less than the fluid and experimental χ, in qualitative agreement with our results. However it was also stated that outside $\eta - \eta_c < (1 + T_i/T_e) L_n/L_s$, the eigenfunctions become more fluid-like, and it was conjectured that experiments have η values on the threshold of that needed for overwhelming fluid transport to ensue. Figure 3 shows that experimental η is never large enough for the fluid eigenfunctions to be valid.

Although linear results are instructive, nonlinear results are needed for experimental comparisons. A renormalization of the fluid propagator equations in the "one point" theory was given in Ref. 10. In this theory, the dominant effect of the nonlinear terms was represented by diffusion-like operators, with turbulent difusion coeffients D_{xx}, D_{yy}, viscosities μ_{xx}, μ_{yy} and mobilities β_{xx}, β_{yy} in terms of the fluctuating field amplitudes. (See Ref. 10 for

exact definitions). It was further argued in Ref. 10–11 that a good estimate for the value of diffusion in steady state can be found as follows. First, replace the $\partial/\partial t$ terms in the mode equations with $-i\omega_r$, where ω_r is the real frequency of the linear eigenode; then solve for D as the complex eigenvalue to make $\gamma = 0$ and use the real part of D for the equilibrium transport. After Fourier transforming in x, one obtains

$$\frac{[-i\omega(1+k_\perp^2)+ik_y(1-Kk_y^2)+k_\perp^2(\mu^{xx}k_x^2+\mu^{yy}k_y^2)+\beta^{xx}k_x^2+\beta^{yy}k_y^2](p+\varphi)}{\{\Gamma[-i\omega(1+k_\perp^2)+ik_y(1-Kk_\perp^2)+k_\perp^2(\mu^{xx}k_x^2+\mu^{yy}k_y^2)+\beta^{xx}k_x^2+\beta^{yy}k_y^2]-ik_y-i\omega-D^{xx}k_x^2+D^{yy}k_y^2\}}$$

$$= (sk_y)^2(-i\omega + D_{xx}k_y^2 + D_{yy}k_y^2)^{-1}\frac{d}{dy}_x(-i\omega + D_{xx}k_x^2 + D_{yy}k_y^2)^{-1}\frac{d}{dk}_x(p+\varphi)\,. \qquad (2)$$

where $s = L_n/L_s$, $K = T_i(1+\eta)/T_e$ and Γ gives the parallel compressibility. After taking $\Gamma = 0$, $s \to 0$ and $k_y \to 0$ (where $\omega_r \to 0$), Eq. (2) is equivalent to the equation quoted in Ref. 9 and 10 (with $z = k_x^3$, and neglecting equilibrium flow). The $s \to 0$ and $k_y \to 0$ limit of Eq. (2) gives $D = 3.26s\,k_y\,K^2$ for the $\ell = 0$ mode and $D = 20s\,k_y\,K^2$ for the $l = 1$ mode.[9] To within a constant multiplier, these formulas are identical to mixing length estimates from the fluid equations as s and $k_y \to 0$.

In Fig. 4 we compare 1) the s and $k_y \to 0$ asymptotic formulas $D = 3.26s\,k_y\,K^2$ for $\ell = 0$ and $D = 20s\,k_y\,K^2$ for $\ell = 1$ 2) numerical solution of Eq. (2) with all terms included for $\ell = 1$, which is the dominant fluid mode 3) values from an interpolation formula for the fluid simulation results in Refs. 12–13 4) gyrokinetic results. (The ratios μ/D and β/D were taken to be 1/2, which is consistent with statements in Refs. 5–6. Also $D^{xx}/D^{yy} = \beta^{xx}/\beta^{yy} = \mu^{xx}/\mu^{yy} = 1$ was used; this is appropriate if the φ spectrum has $k_x \sim k_y$ which is roughly true of the eigenfunction of the full Eq. (2) for $k_y\rho = 0.4$.)

(Also, the fluid simulation interpolation formula is $\chi_{\text{fluid sim}} = (K - K_c)\exp[-4.7s/(K - 5/K)]$, and smoothly combines results in Refs. 12–13; it is valid for $K > 2.5$.)

Several conclusions can be drawn from Fig. 4: 1) the full Eq. (2) gives excellent agreement with the fluid simulation results for experimental s and η; we will therefore regard this χ

as the appropriate result for the fluid equations 2) for experimental parameters, s and the dominant $k_y\rho$ are outside the domain of validity of the asymtotic formulas $D = 3.26s\,k_y\,K^2$ and $D = 20s\,k_y\,K^2$; those formula overestimate the fluid χ for experimental parameters 3) the fluid χ appropriate for experimental parameters is roughly an order of magnitude greater than the gyrokinetic result 4) the asymptotic fluid formula for $s \to 0$ and $k_y \to 0$ and $\ell = 0$ gives χ values 30 or more times larger than the gyrokinetic results.

In Ref. 9, the s and $k_y \to 0$ fluid χ was compared favorably with the kinetic χ at $s = 0.036$; however Fig. 4 shows that these results cannot be extrapolated to experimental s values. Comparisons of the magnitude of the $s \to 0$ and $k_y \to 0$ fluid χ formula and experimental χ are thus highly misleading, and should not be used as a basis for inference about marginal stability.[3,9,15,16,17]

In summary, we conclude that the slab branch of the ITGD instability is too weak to be responsible for transport in L-mode shots. However, other investigators[14,20] have estimated that the toroidal branch can give substantial transport. The gyrokinetic codes used above are being modified to include toroidal effects; preliminary results show that these give much higher transport than the slab case. Thus, the toroidal branch of the ITGD mode deserves consideration as a possible candidate to explain transport.

Acknowledgments

This work was supported by the U.S. Department of Energy contract #DE-FG05-80ET-53088.

References

1. R.J. Groebner *et al.*, Nucl. Fusion **26**, 543 (1986).

2. D.L. Brower *et al.*, Phys. Rev. Lett **59**, 48 (1987).

3. S.D. Scott *et al.*, Phys. Fluids B **2**, 1300 (1990).

4. M. Kotschenreuther *et al.*, to be published in *Plasma Physics and Controlled Nuclear Fusion Research 1990*, Proceedings of the 13th International Conference, Washington D.C..

5. R. Denton and M. Kotschenreuther, to be submitted to J. Comp. Phys.

6. H. V. Wong and P. L. Lyster, in preperation.

7. M. Kotschenreuther, in preperation.

8. G.S. Lee, P.H. Diamond, Phys. Fluids **29**, 3991 (1986).

9. P.W. Terry, *et al.*, Phys Fluids **31**, 2920 (1988).

10. N. Mattor, P.H. Diamond, Phys. Fluids B **1**, 1980 (1989).

11. N. Mattor, P H. Diamond, Phys. Fluids B **2**,1993 (1989).

12. S. Hamaguchi, W. Horton, Phys. Fluids B **2**, 1833 (1990).

13. S. Hamaguchi, W. Horton, Phys. Fluids B **2**, 3040 (1990).

14. M.C. Zarnsdorf *et al.*, to be published in *Plasma Physics and Controlled Nuclear Fusion Research 1990*, Proceedings of the 13th International Conference, Washington D.C.

15. S. D. Scott, P. H. Diamond, *et al.*, Phys. Rev. Lett. **64**, 531 (1990).

16. H. Biglari, P.H. Diamond, *et al.*, *Plasma Physics and Controlled Nuclear Fusion Research 1988*, Proceedings of the 12th International Conference, Nice, Vol. 2 IAEA.

17. N. Mattor and P.H. Diamond, Phys. Fluids B 1, 1981 (1989).

18. R. Lynsker, Phys. Fluids **24**, 1485 (1981).

19. Y.C. Lee, J.Q. Dong, P.N. Guzdar, C.S. Liu, Phys. Fluids **30**, 1331 (1987).

20. F. Romanelli, Lui Chen, and S. Briguglio, Phys. Fluids B **3**, 2496 (1991).

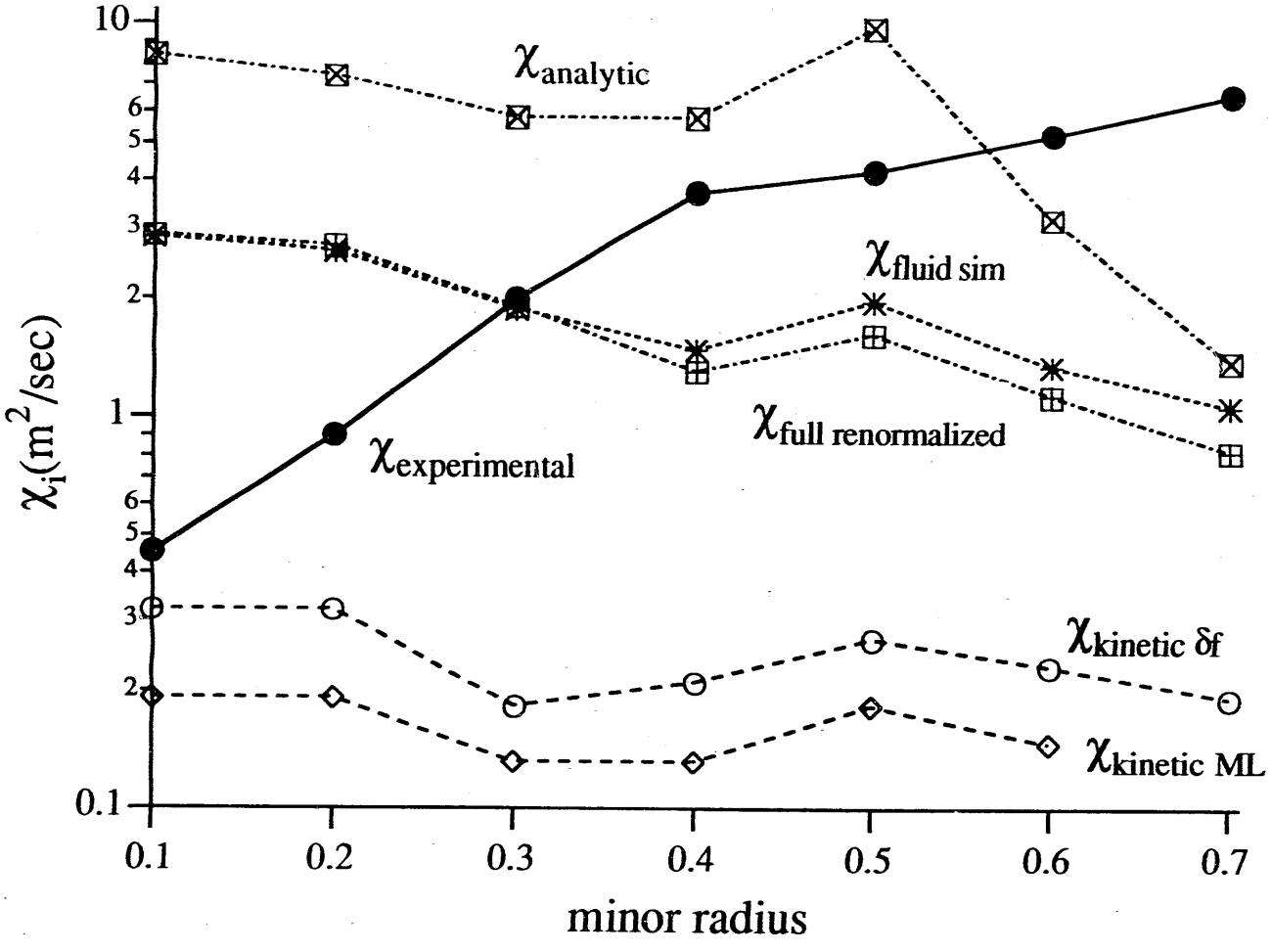

Figure 1. Comparisons if χ_i from experimental data analysis[3], kinetic simulation with the low noise algorithm, kinetic eigenfunction mixing length estimate, fluid simulation[12,13], analytic fluid theory for small s and k_y, and full renormalized equations[10].

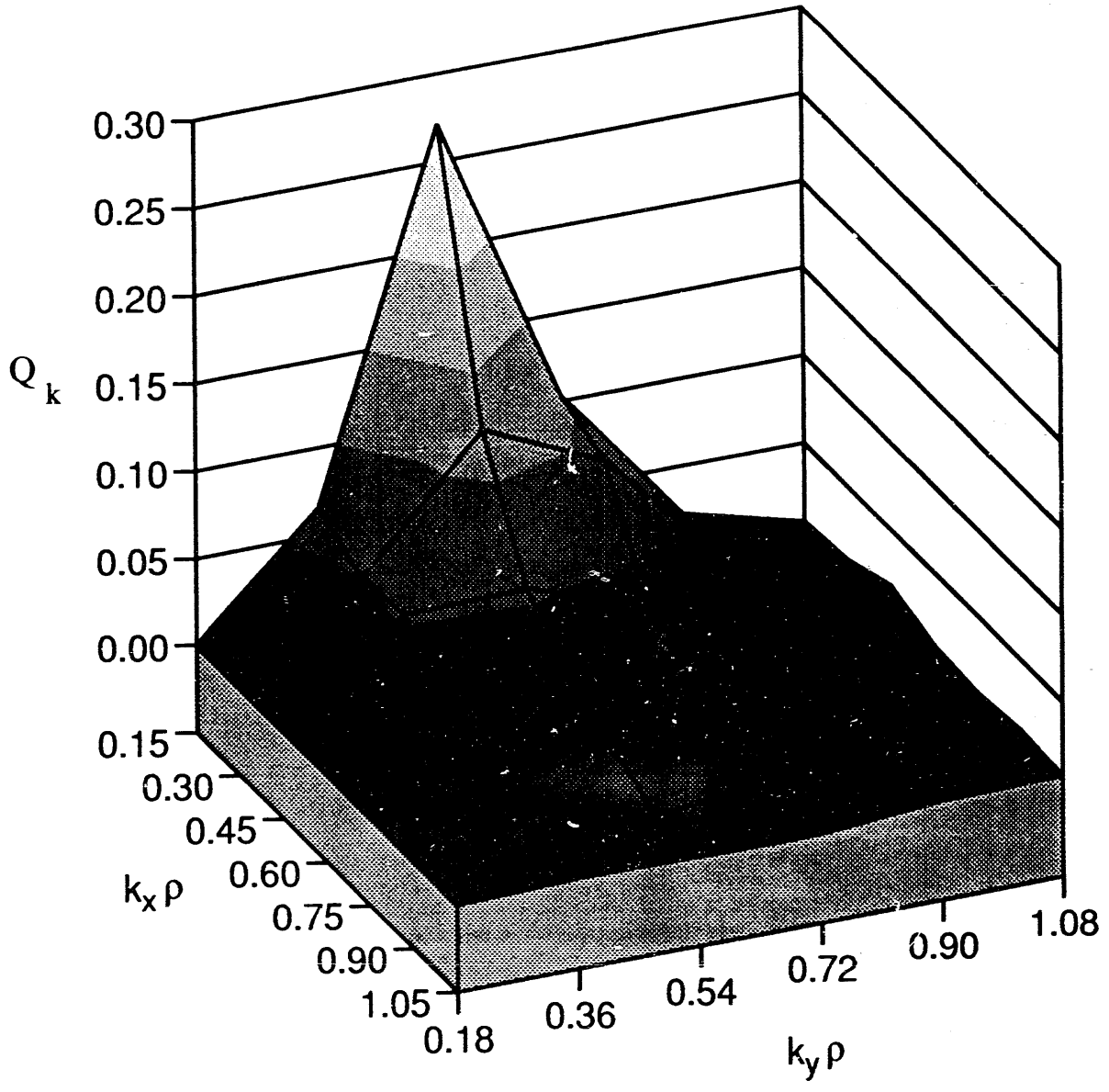

Figure 2. The contributions of the radial and the poloidal components of the heat flux Q_k, for $L_n / L_s = .25$ and $\eta = 5$.

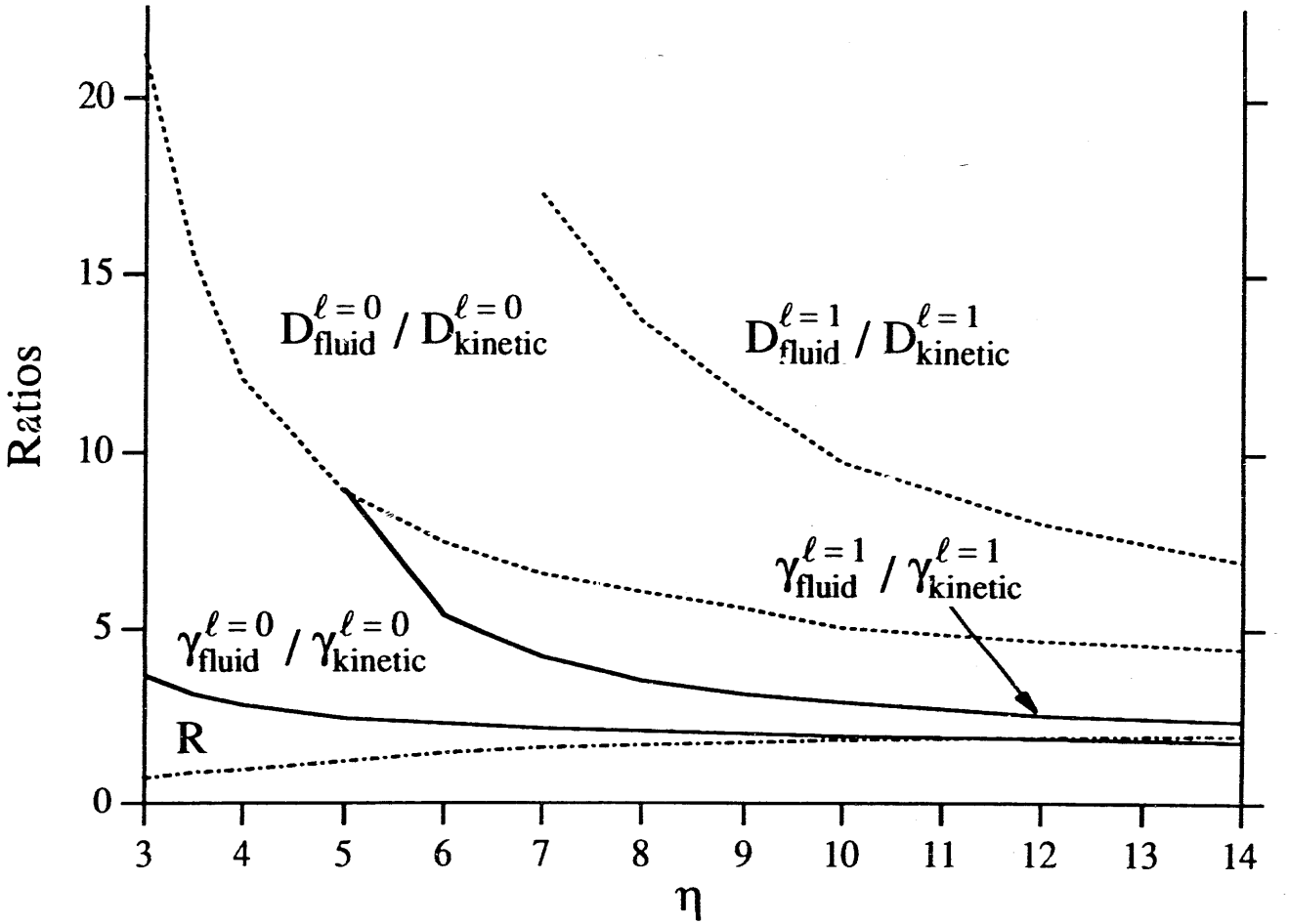

Figure 3. Comparisons of results for ITGD modes in the fluid[8-13] and fully gyrokinetic models for $L_n/L_s = .25$ and $k_y\rho_i = .4$. Shown are ratios of the growth rates and mixing length estimates of diffusion obtained from the linear eigenfunctions for radial mode numbers $\ell = 0$ and $\ell = 1$. Also shown is the ratio, $R = \omega/\langle k_{||}\rangle v$, for the $\ell = 0$ mode.

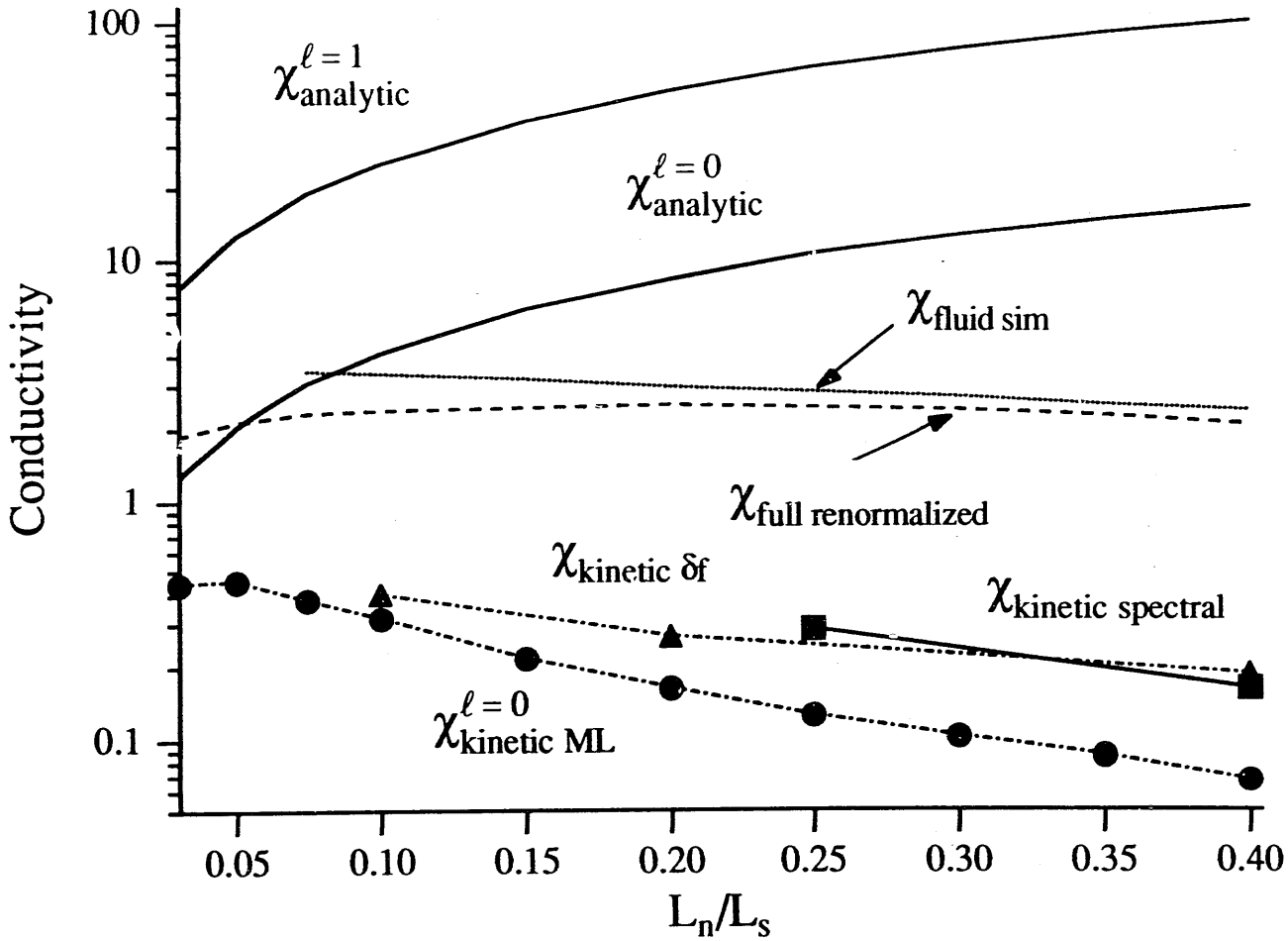

Figure 4. The normalized conductivity vs shear, calculated by various techniques: the kinetic δf particle code, ($\chi_{\text{kinetic }\delta f}$),the kinetic spectral code, kinetic mixing length estimates ($\chi_{\text{kinetic ML}}$), fluid mixing length estimates ($\chi_{\text{fluid ML}}$), χ from fluid simulation ($\chi_{\text{fluid sim}}$), χ from the full "renormalized" equations of ref. 10, and an analytic formula computed for small s and k_y (χ_{analytic_2}).

INSTITUTE FOR FUSION STUDIES
THE UNIVERSITY OF TEXAS AT AUSTIN
RLM 11.218
AUSTIN, TEXAS 78712-1060
U.S.A.

END

DATE
FILMED
2/26/92